Naval Research Laboratory

Washington, DC 20375-5000

NRL Memorandum Report 6443

The Inadequacies of Damage Energy as a Measure of Displacement Damage

GEORGE P. MUELLER

Condensed Matter and Radiation Sciences Division

April 10, 1989

SECURITY CLASSIFICATION OF THIS PAGE

REPORT DOCUMENTATION PAGE

Form Approved
OMB No. 0704-0188

1a. REPORT SECURITY CLASSIFICATION UNCLASSIFIED	1b. RESTRICTIVE MARKINGS
2a. SECURITY CLASSIFICATION AUTHORITY	3. DISTRIBUTION/AVAILABILITY OF REPORT Approved for public release; distribution unlimited.
2b. DECLASSIFICATION/DOWNGRADING SCHEDULE	
4. PERFORMING ORGANIZATION REPORT NUMBER(S) NRL Memorandum Report 6443	5. MONITORING ORGANIZATION REPORT NUMBER(S)
6a. NAME OF PERFORMING ORGANIZATION Naval Research Laboratory 6b. OFFICE SYMBOL (If applicable) Code 4601	7a. NAME OF MONITORING ORGANIZATION
6c. ADDRESS (City, State, and ZIP Code) Washington, DC 20375-5000	7b. ADDRESS (City, State, and ZIP Code)
8a. NAME OF FUNDING/SPONSORING ORGANIZATION 8b. OFFICE SYMBOL (If applicable)	9. PROCUREMENT INSTRUMENT IDENTIFICATION NUMBER
8c. ADDRESS (City, State, and ZIP Code)	10. SOURCE OF FUNDING NUMBERS PROGRAM ELEMENT NO. / PROJECT NO / TASK NO / WORK UNIT ACCESSION NO DN157-033

11. TITLE (Include Security Classification)
The Inadequacies of Damage Energy as a Measure of Displacement Damage

12. PERSONAL AUTHOR(S)
Mueller, G.P.

13a. TYPE OF REPORT	13b. TIME COVERED	14. DATE OF REPORT (Year, Month, Day)	15. PAGE COUNT
Interim	FROM _____ TO _____	1989 April 10	30

16. SUPPLEMENTARY NOTATION

17 COSATI CODES			18. SUBJECT TERMS (Continue on reverse if necessary and identify by block number)
FIELD	GROUP	SUB-GROUP	Displacement Damage energy

19. ABSTRACT (Continue on reverse if necessary and identify by block number)

The Lindhard, Nielsen, Scharff and Thompson equations for the partitioning of an ion's energy into electronic and damage portions are widely used to estimate the number of displacements produced in a solid by an impinging ion. We have extended the LNST approach by including a threshold displacement energy at all stages of the calculation, which allows us to form an integral equation that yields the number of displacements $N_V(E)$ directly, rather than estimating it from the damage energy D(E). We compare our results with both the LNST approach and with the collision simulation code MARLOWE. We find that our approach approximates the MARLOWE results reasonably well, but that the damage energy is a poor estimator of displacement damage, because $N_V(E)$ and D(E) have different dependencies on the interatomic potential and on the low energy portion of the inelastic loss function.

20. DISTRIBUTION/AVAILABILITY OF ABSTRACT ☒ UNCLASSIFIED/UNLIMITED ☐ SAME AS RPT ☐ DTIC USERS	21. ABSTRACT SECURITY CLASSIFICATION UNCLASSIFIED
22a. NAME OF RESPONSIBLE INDIVIDUAL G.P. Mueller	22b. TELEPHONE (Include Area Code) (202) 767-6977 22c. OFFICE SYMBOL Code 4601

DD Form 1473, JUN 86 *Previous editions are obsolete.* SECURITY CLASSIFICATION OF THIS PAGE

S/N 0102-LF-014-6603

CONTENTS

THE INADEQUACIES OF DAMAGE ENERGY AS A MEASURE OF DISPLACEMENT DAMAGE

INTRODUCTION

One of the few simple measures of radiation damage that relates damage in crystals at the microscopic level to the gross behavior of the material is the number of Frenkel pairs produced by a given irradiation. Even though a significant fraction of the pairs initially produced quickly recombine, the expectation is that the number of vacancies produced by an irradiation is a rough indication of the extent of permanent damage to the material. Currently there is interest in the calculation of displacement damage because of the apparent relationship between the number of displacements produced by an impinging ion and the damage suffered by semiconductor materials and devices.[1,2]

The underpinning of calculations of radiation damage is a model of the isolated displacement event. Suppose an ion of charge Z_1e and mass A_1 is moving with energy E in a material and collides with a lattice atom of charge Z_2e and mass A_2, transferring an energy T to the bound atom. The conditions under which a struck atom leaves its native site depends on the momentum of the impinging ion, on the crystal structure of the material and on the form of the potential that holds the material together. A number of general discussions of displacement effects are available (Dienes and Vineyard,[3] Sosin and Bauer,[4] Robinson,[5] Lehmann,[6] Gittis,[7] Averback and Kirk[8])

To delineate our displacement model, we define a series of energy parameters. Let E_D be the displacement energy; if T is less than E_D, then the struck atom stays in place and shares its newly gained energy with the lattice, but if $T>E_D$, then the struck atom is displaced and procedes to move through the crystal. (In reality the displacement energy in a crystal depends on direction, but we assume an isotropic value.) Further, if the incoming ion transfers an energy $T>E_D$, but retains an energy $E-T<E_D$, then it replaces the struck atom at the lattice site--no vacancy is produced. If more than one species is present in the calculation, the role of replacements is more complicated.)

We next allow a binding energy E_B. If a vacancy is produced, the displaced atom retains energy $T-E_B$; the binding energy E_B is accounted for by the relaxation of the lattice atoms surrounding the vacancy. We assume that $E_B<E_D$ and that the effect of the binding energy is assessed after the collision. For example, if $T>E_D$, then there is a displacement even though it may be the case that $T-E_B<E_D$. Finally, we presume there are no binding losses in replacement collisions.

Manuscript approved January 29, 1989.

We will follow the course of Robinson and Torrens[9] in their binary-collision simulation code MARLOWE by defining a cutoff energy E_C; ions moving with energies less than E_C are considered to have stopped. This concept is useful in simulation calculations because it saves the time necessary to follow the numerous, but ineffectual, slowly moving ions. While such a cutoff has no particular benefit for analytical displacement calculations, we retain it so as to ease comparisons of our work with the simulation models. We will use the values $E_C = 0$, E_D, $2E_D$.

Some of an ion's initial energy E, a portion labeled I(E), will go toward exciting the electrons in the solid. Robinson and Torrens categorize the bins into which the remaining energy falls as follows: binding energy loss B(E), as discussed above; remaining kinetic energy, the energy retained by ions moving with energies less than E_C; and subthreshold loss, energies less than E_D acquired by (undisplaced) lattice atoms. We will combine the last two quantities into one, which we call the thermal loss H(E). Thus we have

$$E = I(E) + D(E) = I(E) + B(E) + H(E) \qquad (1$$

The quantity D(E) is usually called the damage energy, which by definition is all the energy not lost to inelastic processess.

Robonson and Oen[10] point out that some of the subthreshold energy is lost to inelastic processes, so that our I(E) should be somewhat larger and H(E) somewhat smaller. This effect has no consequence for our principal results, which depend on the direct calculation of the number of displacements without using the damage energy as an intermediate step. Their modification would make some difference in our estimates of damage energy, but, as discussed later, the concept of inelastic losses at very low energies is of dubious value.

In the early calculations of displacement damage[11] the inelastic loss was not specifically included. Instead, the partition was often made that all of an ion's energy above some value E_I was lost to the electrons, while all of its energy below this value went into creating displacements by means of elastic collisions; that is, the damage energy was E for $E<E_I$ and E_I for $E>E_I$. As the calculations became more sophisticated, the inelastic losses were included throughout the calculation. The loss I(E) to the electrons could be directly calculated, but the remaining energy was still called the damage energy. It is not obvious, given the simultaneous inelastic losses as the displacements are produced, that there is a direct relation between the damage energy and the number of displacements. The examination of this point is the main goal of this report.

Several other assumptions should be pointed out. For a lattice atom that is given energy $T<E_C$, we assume that all of the energy T goes into the thermal energy bin H(E). For bound or captured ions with kinetic energies less than E_D, we assume all of the energy is lost thermally, even if these energies are greater than E_C.

Turning specifically to displacement mechanisms, as opposed to energy loss mechanisms, we note that an ion moving in a crystal with energy less than E_D can produce neither replacements nor vacancies. If the ion has an energy between E_D and $2E_D$, it cannot produce a vacancy, but

may generate a replacement collision. Figure 1 summarizes the collisional possibilities of our model. Starting with a zero cutoff energy in fig. 1a, we see the thermal loss, vacancy production and replacement regions of the E-T,T plane. For an ion of energy E ($E=5.4E_0$ in this example), all of its possible (elastic) collisions lie on the dashed 45 degree line. In fig. 1b we impose the cutoff $E_C=E_0$. We presume that all ions of energy less than the cutoff lose their energy to thermal processes; specifically, there are no electronic losses in the cutoff (C) region. We see that the only difference in $E_C=0$ and $E_C=E_0$ calculations is in the relative amounts of thermal and electronic

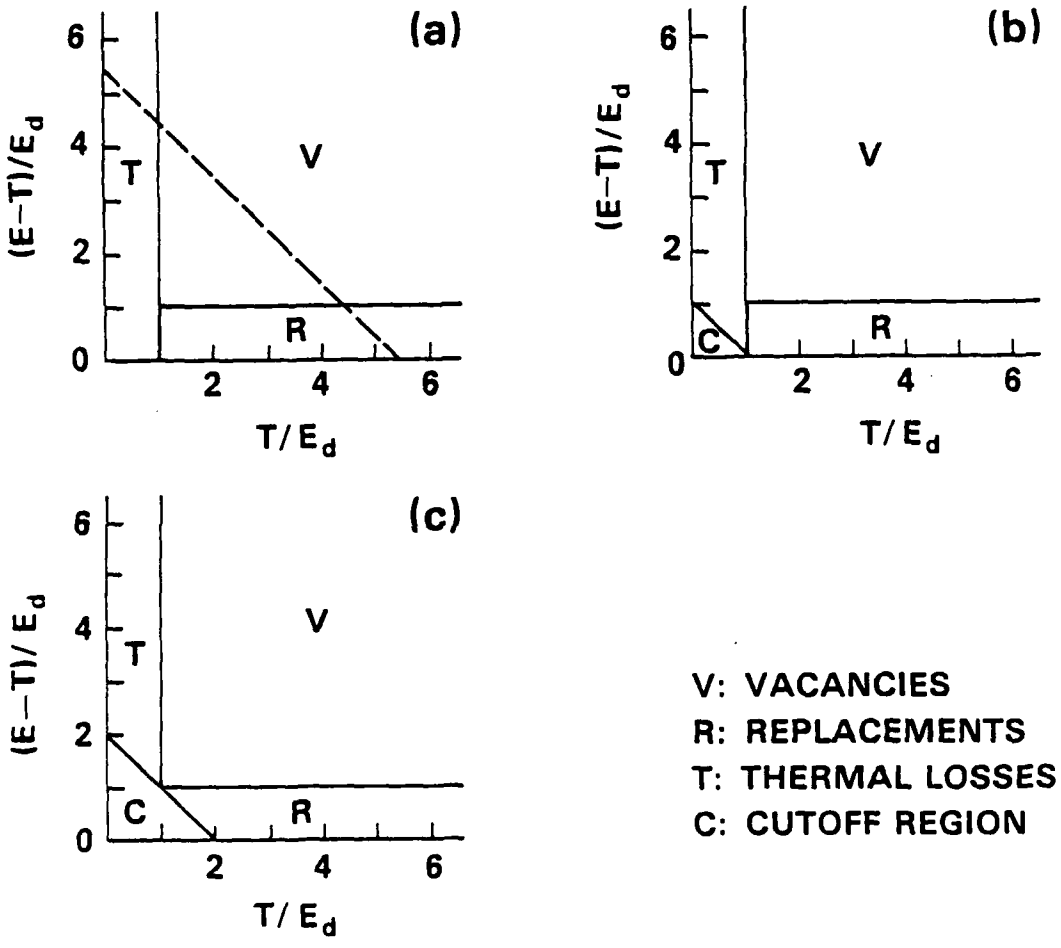

Fig. 1 -- The various collision possibilities as a function of energy transfered and energy retained; shown for cutoff energies of a) $E_C=0$, b) $E_C=E_0$ and c) $E_C=2E_0$. The thermal loss, replacement producing, vacancy producing, and cutoff regions are shown. See the text for a detailed discussion.

loss. As we view the case $E_C=2E_D$ in fig. 1c we note a further shift in the relative thermal and inelastic losses. A cutoff of $2E_D$ also reduces the estimated number of replacements, because some ions that would undergo replacement collisions are no longer followed.

Almost all displacement calculations have assumed that the initial ion, of energy $E>E_D$, is itself a displacee--produced, for example, by an incident neutron. If N(E) is the average number of vacancies resulting from an ion of energy E, then this initial displacement assumption amounts to the requirement that

$$N(E) = \begin{cases} 0, & E < E_D \\ 1, & E_D < E < 2E_D \end{cases} . \qquad (2$$

We find it more natural to assume the cascade starts with an ion of energy E moving freely in the crystal and to calculate the number of secondary vacancies that are produced, which we call $N_V(E)$. For the monatomic substances that we consider, we find--it follows from the integral equation--that $N_V(E)=0$ for $E<2E_D$. The two estimates of displacement damage are related by $N(E)=N_V(E)+1$ for $E>E_D$.

The earlier calculations of displacement damage involved solving an integral equation[3] for N(E). More recently, the LNST (Lindhard, Nielsen, Schraff and Thompsen)[12] results for the damage energy D(E) (see Sigmund[13] for a brief history of their approach) have been widely used to estimate displacement damage through the use of the Khinchin-Pease formula

$$N(E) = \kappa\, D(E) / (2\, E_D) , \qquad (3$$

where κ is a constant of the order[14] of 0.8. In our approach we return to a direct calculation of N(E). Because we also calculate D(E), we can compare the two approaches and judge the worth of the damage energy approximation for estimating displacement damage.

In the next two sections we lay out the formalism that leads to integral equations for $N_V(E)$, H(E), B(E), I(E), which we have discussed, and $N_R(E)$, the number of replacements produced by an ion of energy E. We compare our results first with the binary-collision simulation code MARLOWE,[9] and then with the standard analytical transport theory of LNST. All of the numerical results in this paper and much of the discussion assume a monoatomic crystal; the extention to complex substrates is straightforward, but does not affect the points made here.

An preliminary version of this work was reported some time ago.[15] At about the same time, Coulter and Parkin[16] independently investigated some of these same questions.

CROSS SECTIONS AND STOPPING POWERS: GENERAL FORMS

Let the differential cross section $\Phi(E,T)dT$ represent all of the scattering processes that an ion can undergo, wherein the ion retains energy E-T and transfers energy T to some other particle in the solid. The total scattering cross section is given by

$$\Phi(E) = \int_0^E dT\ \Phi(E,T) \qquad (4$$

We suppose that $\Phi(E,T)$ is composed of four additive parts,

$$\Phi(E,T) = \Phi_E(E,T) + \Phi_N(E,T)$$

$$= \Phi_E(E,T) + \Phi_T(E,T) + \Phi_R(E,T) + \Phi_V(E,T)\ , \qquad (5$$

representing the following types of collisions: electronic, thermal, replacement, and vacancy, respectively. The last three are all portions of the elastic scattering cross section $\Phi_N(E,T)$, as pictured in fig. 1.

The electronic cross section is $\Phi_E(E,T)dT$, where T represents the sum of the energies transferred from the moving ion to the electrons of the lattice atom. All of this energy goes into inelastic losses; no displacements are produced. In the rest of this paper we will have need only for the electronic stopping power, given by

$$S_E(E) = \int_0^E dT\ T\ \Phi_E(E,T)\ , \qquad (6$$

and not for the cross section itself.

For the thermal losses we write

$$\Phi_T(E,T)\,dT = \Phi_N(E,T)\ U(E_D-T)\ dT\ , \qquad (7$$

where U( ) is the unit step function and Φ_N is the macroscopic, elastic scattering, differential cross section. We define a quantity that we call the thermal stopping power,

$$S_T(E) = \int_0^E dT\ T\ \Phi_N(E,T)\ U(E_D-T)\ , \qquad (8$$

which is analogous to the electronic stopping power.

The replacement and vacancy cross sections are

$$\Phi_R(E,T)dT = \Phi_N(E,T)\ U(E_D-(E-T))\ U(T-E_D)\ dT \qquad (9$$

and

$$\Phi_V(E,T)dT = \Phi_N(E,T)\ U(T-E_D)\ U(E-T-E_D)\ dT\ . \qquad (10$$

The total cross sections for the replacement, vacancy and thermal processes are given by

$$\Phi_i(E) = \int_0^E dT\, \Phi_i(E,T)\,, \qquad i=R,V,T; \tag{11}$$

and we set

$$\Phi_{RV}(E) = \Phi_R(E) + \Phi_V(E)\,. \tag{12}$$

In the same spirit that we defined the electronic stopping power and the thermal stopping power, we define a binding energy stopping power, given by

$$S_B(E) = E_B\, \Phi_V(E)\,, \tag{13}$$

and a replacement stopping power, which represents the kinetic energy retained by the replacements as they are bound onto lattice sites, given by

$$S_R(E) = \int_0^E dT\ (E-T)\ \Phi_R(E,T)\,. \tag{14}$$

DERIVATION OF THE INTEGRAL EQUATIONS

The following discussion parallels the approach of LNST.[12] Suppose that we are interested in some physical process, such as the average number of vacancies $N_V(E)$ that an ion of energy E will produce. Suppose the ion undergoes a collision that results in its retaining an energy E-T and transferring energy T to some other particle in the solid. These two particles will traverse the solid producing more vacancies; we measure the extent of these effects by $N_V(E-T)$ and $N_V(T-E_R)$, where $E_R=E_B$ when a vacancy is produced and $E_R=0$ otherwise. In addition, a vacancy may be induced at the collision site itself. We measure this collision dependent effect with the function $N_V(E,T)$, which will be either zero or one.

Because some such collision is part of the natural chain of events that leads our original particle to produce a number $N_V(E)$ of vacancies, we know that, on the average, the effect of $N_V(E-T)$, $N_V(T-E_B)$ and $N_V(E,T)$ must be the same as that of the incoming ion. By averaging over the collisional possibilities, we can express this equality as

$$\Phi(E)\, N_V(E) = \int_0^E dT\ \Phi(E,T)\ [\, N_V(E-T) + N_V(T-E_R) + N_V(E,T)\,]\,. \tag{15}$$

One can find more detailed derivations of eq. (15) in LNST and elsewhere (Sigmund et al,[17] Winterbon, Sigmund and Sanders[18] (WSS)), but in substance they reduce to this balancing

argument.

If we split the cross section into its four components and replace the total cross section $\Phi(E)$ by its integral form, we obtain

$$0 = \int_{E-E_D}^{E} dT\ \Phi_R(E,T)\ [\ N_V(E) - N_V(T) - N_{V,R}(E,T)\ ]$$

$$+ \int_{E_D}^{E-E_D} dT\ \Phi_V(E,T)\ [\ N_V(E) - N_V(E-T) - N_V(T-E_B) - N_{V,V}(E,T)\ ]$$

$$+ \int_{0}^{E_D} dT\ \Phi_t(E,T)\ [\ N_V(E) - N_V(E-T) - N_{V,T}(E,T)\ ]$$

$$+ \int_{0}^{E} dT\ \Phi_E(E,T)\ [\ N_V(E) - N_V(E-T) - N_{V,E}(E,T)\ ]\ , \qquad (16$$

where we have let $N_{V,j}(E,T)$ represent the number of vancancies produced at the collision site when the j (j=V,R,T,E) cross section is operative. Only a vacancy producing collision results in a non-zero value of $N_{V,j}(E,T)$, j=V,R,T,E, so that

$$N_{V,V}(E,T) = 1$$
$$N_{V,j}(E,T) = 0\ ,\ j=R,T,E. \qquad (17$$

In eq. (16) LNST would have replaced $N_V(T-E_B)$ by $N_V(T)$, because E_B is small compared to the other energies and because they were not interested in the effects of a binding energy. We will keep the E_B parameter, although we often set its value to zero. We now make use of an approximation of LNST: that the energy transfer in electronic collsions is small compared to the energy of the scattered ion. For $N_V(E-T)$ they would write

$$N_V(E-T) \approx N_V(E) - N_V'(E)\ T \qquad (18$$

in the integral with the electronic cross section, so that the first two integrals in the last line of eq. (16) are replaced by $S_E(E)\ N_V'(E)$. We also impose approximation (18) on the thermal collisions, so that the integral of the first two terms in the third line of eq. (16) is replaced by $S_T(E)\ N_V'(E)$. Because the energy transferred in a thermal scattering is, by definition, less than E_D, the relation (18) will be a good approximation in thermal collisions except, possibly, for energies $E<E_D$. We show, in Appendix B, that this approximation is warranted. For convenience, we call these the electronic stopping power and thermal stopping power approximations.

When we make use of the various definitions of cross sections and stopping powers that

appear in the previous section and adopt these two approximations, we can write our integral equation in the form

$$[\, S_E(E) + S_T(E) \,]\, N_V'(E) \;+\; \Phi_{RD}(E)\, N_V(E) \;+\; J_V(E) \;=\; G_V(E) \tag{19}$$

where $G_V(E)$ is the integral expression

$$G_V(E) = \int_0^E dT \,\{\, \Phi_R(E,T)\, N_V(T) \;+\; \Phi_V(E,T)\, [\, N_V(E-T) + N_V(T-E_B) \,] \,\}, \tag{20}$$

and $J_V(E)$ is the inhomogeneous term

$$J_V(E) = -\Phi_V(E). \tag{21}$$

In exactly the same manner (see Appendix A) we can derive integral equations for the quantities N_R, B, H, and I. We solve these integral equations numerically using a cubic spline method.[19]

COMPARISON WITH BINARY-COLLISION SIMULATIONS

The best, readily available, method of calculating displacement damage is the binary-collision simulation code MARLOWE,[9] which simulates radiation effects by following individual ions through a psuedo crystal. Among the many differences between the simulation code MARLOWE and the present, analytical transport theory, approach are the following:

a) MARLOWE models a crystalline material, instead of treating the substrate as amorphous.

b) MARLOWE calculates the exact scattering angles and energy transfers for each collision using the Molière potential.[20] This potential is a version ofthe Thomas-Fermi potential with an exponential tail and is thought to be more realistic.[21] The present theory uses an approximate cross section[22] based on the Molière potential, which is obtained by using the same approximations[23] that Lindhard, Nielsen and Scharff[24] (LNS) use to obtain their cross section from the Thomas-Fermi potential. The detailed forms of the Molière potential and cross section can be found in Appendix C.

c) With MARLOWE one has a choice of inelastic loss mechanisms. Several differential cross sections for electronic loss are built into the code, as is a nonlocal, continuous slowing down, model of electronic loss. The present analytical method incorporates only a continuous slowing down model that is similar, but not identical to, that used in MARLOWE.

d) MARLOWE imitates the effects of many body collisions by allowing, in a fashion, several binary collisions to occur simultaneously.

e) MARLOWE imposes a cutoff in the maximum impact parameter for which a collision, elastic or inelastic, may occur.

f) MARLOWE remembers previous damage, so that, if the cascade doubles back on inself, the same lattice atom cannot be removed from its lattice site twice. The analytical code is essentially an ensemble average, each (figurative) element of which sees only virgin substrate.

As the first stage of comparison, we want to eliminate as many of these differences as possible. In particular, if we could turn all of them off, and if we then found that the two calculations gave similar results, we could examine the effect of each dissimilarity by selectively turning it back on.

We examine the case of an fcc copper crystal. For the screening length that appears in the Molière potential we use the value a=7.38 pm.[25] For the energy parameters discussed in the introduction we use E_B=0 and E_C=E_D=25 eV. In order to effect the comparison, we make the following modifications and adjustments to MARLOWE:

a) We run MARLOWE in its amorphous mode, in which the crystal is rotated through some random angle after each scattering. This has the effect of imitating, if not duplicating, the amorphous character of the analytical code.

b) We insert into MARLOWE a new scattering angle subroutine that simulates the effect of the approximate cross section that the analytical code uses. In Appendix C we indicate how to start with the approximate Molière cross section and obtain the scattering angle versus impact parameter relation that we use in MARLOWE.

c) We turn off the inelastic stopping in both codes. Because of the conceptual differences in the two models of inelastic loss, there is no simple way to make them comparable. In any case, we are not interested at the moment in differences in displacement damage caused by different electronic loss models.

d) We make use of a MARLOWE provision that allows the simultaneous collision feature to be turned off.

To a greater or lesser extent these modifications remove the major dissimilarities between the two approaches.

For the moment we ignore differences (e) and (f), as well as any others that we have not identified. In order to compare the two approaches we plot the displacement efficiency as a function of energy. The displacement efficiency $K_V(E)$ is defined in terms of the total number of displacements by

$$N(E) = K_V(E)\, D(E) / 2E_D \,. \qquad (22$$

The quantity $K_V(E)$ measures the efficiency with which vacancies are produced relative to the hard core model, for which $K_V(E)$=1. Because we have turned off the inelastic losses, all of the

energy is damage energy, so that D(E)=E.

In fig. 2 we show that displacement efficiency for the present theory, for MARLOWE with the changes listed above and for a straight MARLOWE calculation modified only by the absence of inelastic losses. We see that the agreement between the present theory and the modified MARLOWE results is quite good. Both approaches indicate that the displacement efficiency becomes constant at 0.5-1.0 keV. For the standard MARLOWE calculation there is more structure in the displacement efficiency curve due to the effects of the lattice. The more realistic MARLOWE calculation indicates a somewhat (9 percent) higher displacement efficiency above 1 keV.

To study the exact origin of this difference, we start with the standard MARLOWE

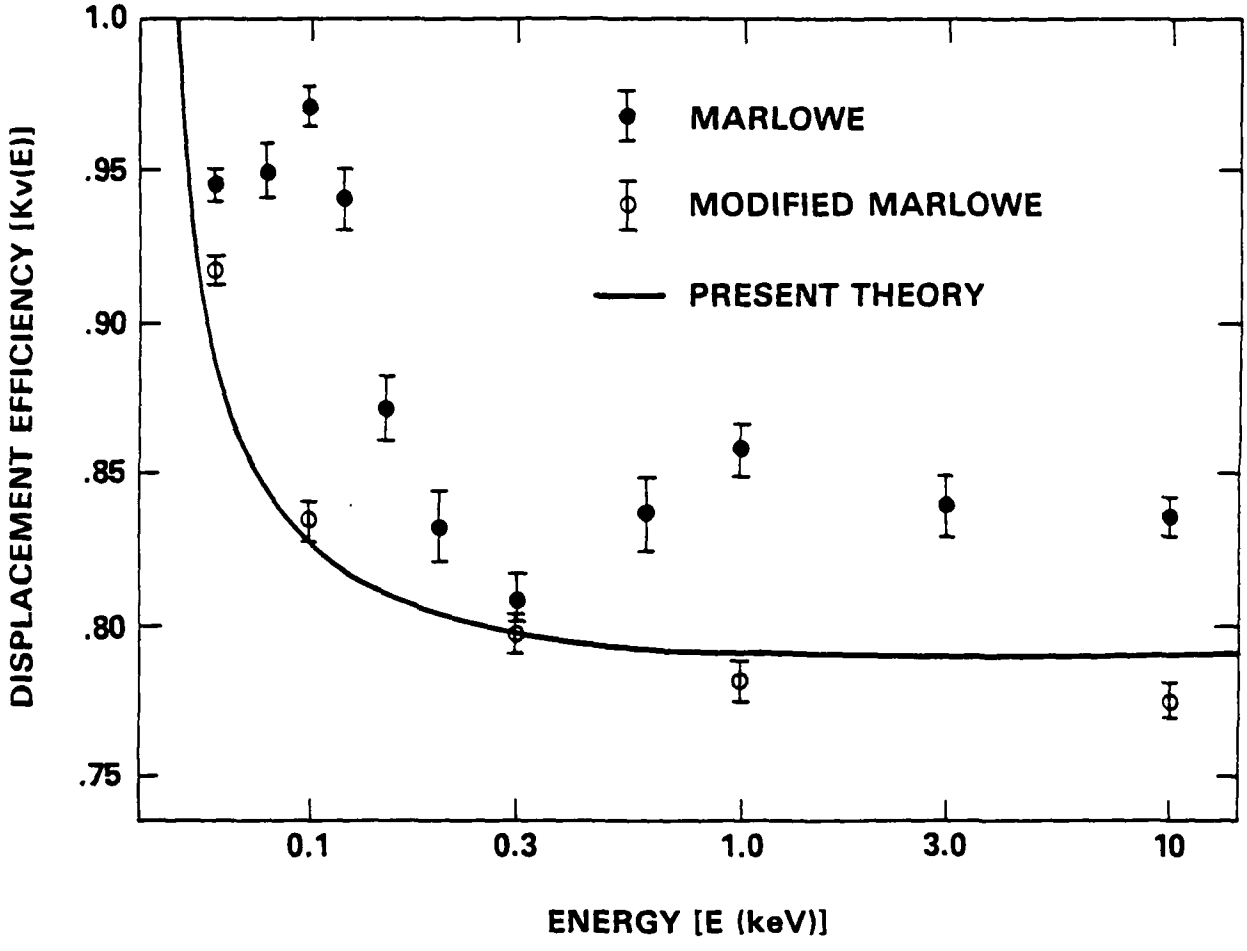

Fig. 2 -- A comparison of displacement efficiency as estimated by the present theory, MARLOWE, and MARLOWE as modified to contain some of the same approximations as the present theory. (The case shown is for fcc copper with Ed=25 eV and no inelastic losses.)

calculation, at E=1 kev, and selectively turn on various combinations of approximations. Table 1 shows the results of this procedure. We see that the effects of the different approximations are not additive. The only consistent effect seems to be that an amorphous substrate tends to reduce the number of vacancies by 5-10 percent.

Table 1 -- Effect of Various Approximations on the Number of Vacancies

Approximations Added to the Standard MARLOWE Calculation			Percentage Change in N(E) at 1 keV
Amorphous Substrate	Isolated Collision	WSS Cross Section	
-	-	-	--
-	X	-	+1
-	-	X	+3
-	X	X	0
X	-	-	-4
X	X	-	-5
X	-	X	-11
X	X	X	-9

We can compare the efficiency with which replacements are produced in the same manner in which we examined vacancies. We define a replacement efficiency

$$N_R(E) = K_R(E)\, D(E) / 2E_D \,. \qquad (23$$

Using the same assumptions, we again have D(E)=E. We see in fig. 3 that the present results are somewhat lower but of the same pattern as the amorphous, WSS cross section, isolated collision, version of MARLOWE. But the effect of neglecting the crystal structure is large in this case, as one might expect; the present results are only 30 percent of the straight MARLOWE results.

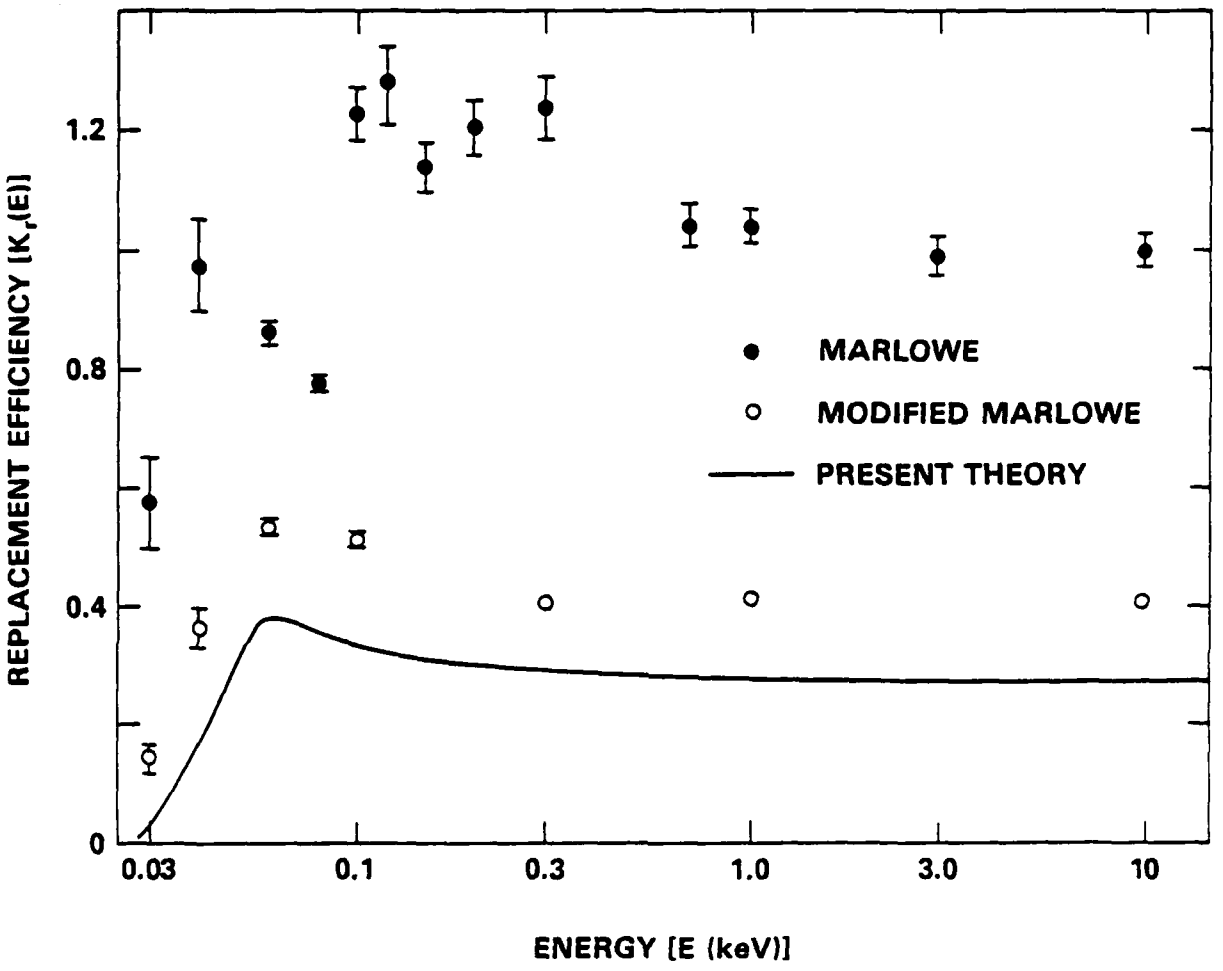

Fig. 3 -- A comparison of replacement efficiency shown for the same conditions as the last figure.

COMPARISON OF DAMAGE ENERGY ESTIMATES

Comparisons of the present approach and MARLOWE are difficult when electronic losses are included. We use the LNST continuous slowing down model (see eq. (C15)); the Firsov stopping power coefficient has the value k=0.2077 $ev^{1/2}$ $Å^{-1}$ for copper. The energy loss process is applied continuously in the differential equation so that, figuratively, each moving ion continuously undergoes inelastic losses. MARLOWE can also use this non-local stopping law, but it is applied to the line segments that are generated by the elastic collision asymptotes. At low energies, especially, there are a number of differences in the two methods.

MARLOWE also can use a local electronic loss mechanism, with a differential cross section of exponential form, such that the stopping power resulting from that cross section is essentially the same as that of the continuous slowing down model. In fig. 4 we show the results of MARLOWE runs with both stopping mechanisms and the results of the present approach. At low energies there is notable disagreement between them. At higher energies the local stopping

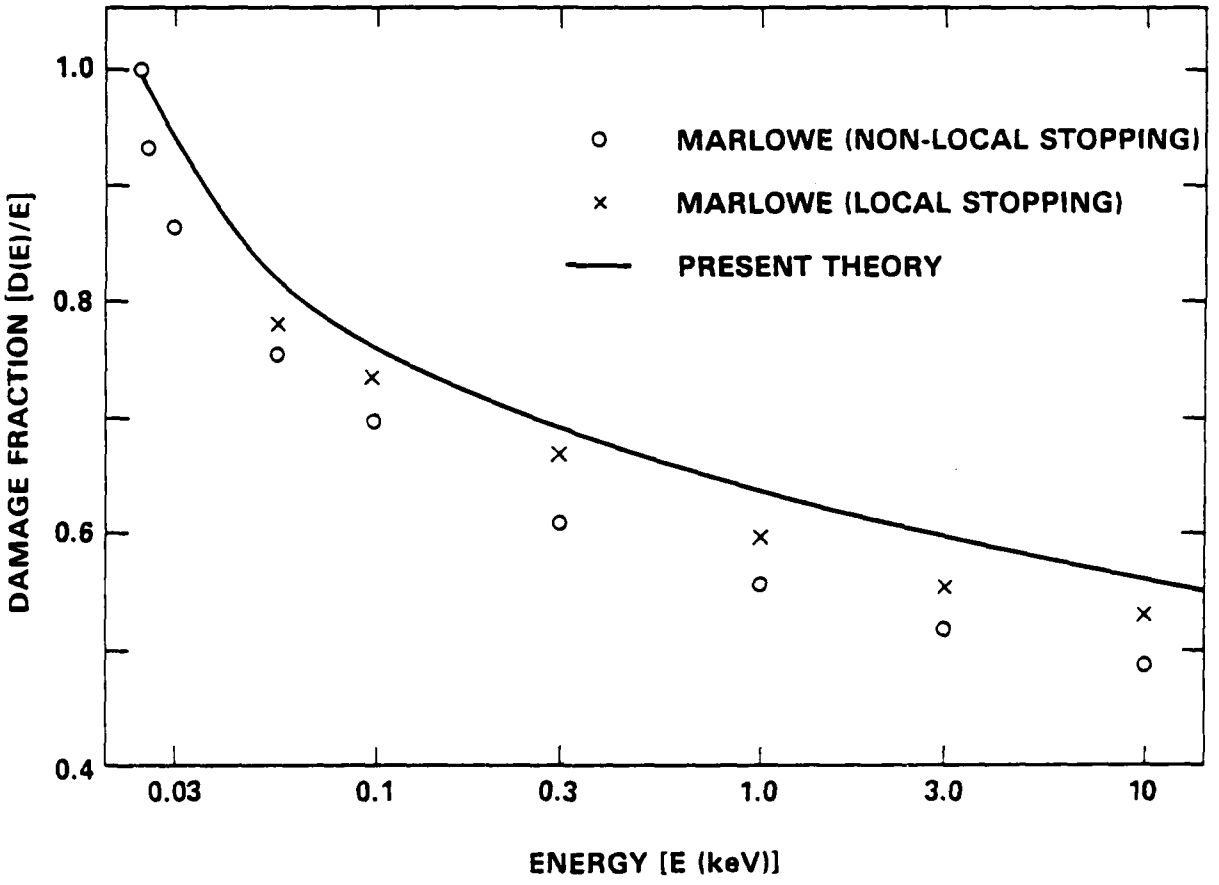

Fig. 4 -- A comparsion of the damage fraction (D(E)/E) for the same conditions as fig. 2, except that inelastic losses are included.

method in MARLOWE agrees more closely with the present approach than with the other MARLOWE model. We conclude that differences in the models preclude good agreement in estimates of damage energy.

EFFECT OF POTENTIAL

The conventional LNST energy partitioning theory is based on the Thomas-Fermi interaction. Figure 5 serves to demonstrate the effect on energy partitioning of changing the interaction. All of the curves are based on the formalism of this paper. The solid curve represents the results of using the WSS[18] fit to the LNS[24] version of the Thomas-Fermi cross section, with the Lindhard screening length a=10.78 pm. (The details of these interactions and the expressions for the screening lengths are given in Appendix C.) The two dashed curves represent

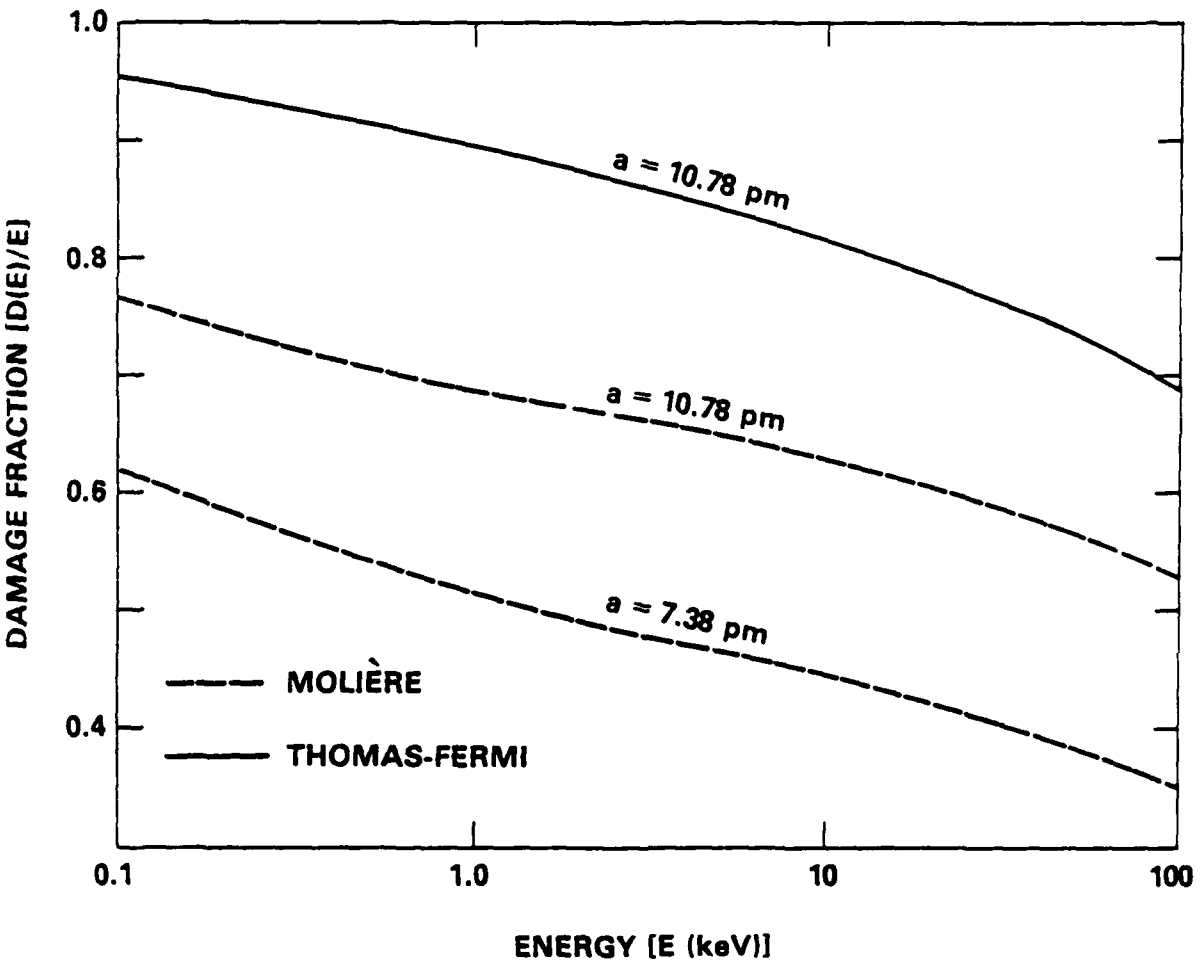

Fig. 5 -- A comparison, using the present theory, of the damage fraction in copper using three different cross sections.

the results of using the cross section based on the Molière potential, both for the Lindhard value of the screening length and the Torrens and Robinson[25] value a=7.38 pm, which was obtained by adjusting the screening length so that the low energy portion of the Molière potential agreed with a Cu-Cu interaction that reproduced some of the bulk properties of copper. We see that there are large shifts away from the LNST (Thomas-Fermi interaction with LNST screening length) in the damage energy, produced by switching from the Thomas-Fermi to the more realistic Molière potential, and then produced by switching to the smaller, more realistic, screening length.

We can make another comparison of the effects of changing the potential be examining the number of vacancies produced in each case. In fig. 6 we plot the number of vacancies produced per unit energy (N(E)/E) as a function of energy. The two potentials that use the 10.78 pm screening length are in rough agreement at all energies, presumably because the Thomas-Fermi and Molière cross sections coincide for higher relative energy transfers. Upon comparing

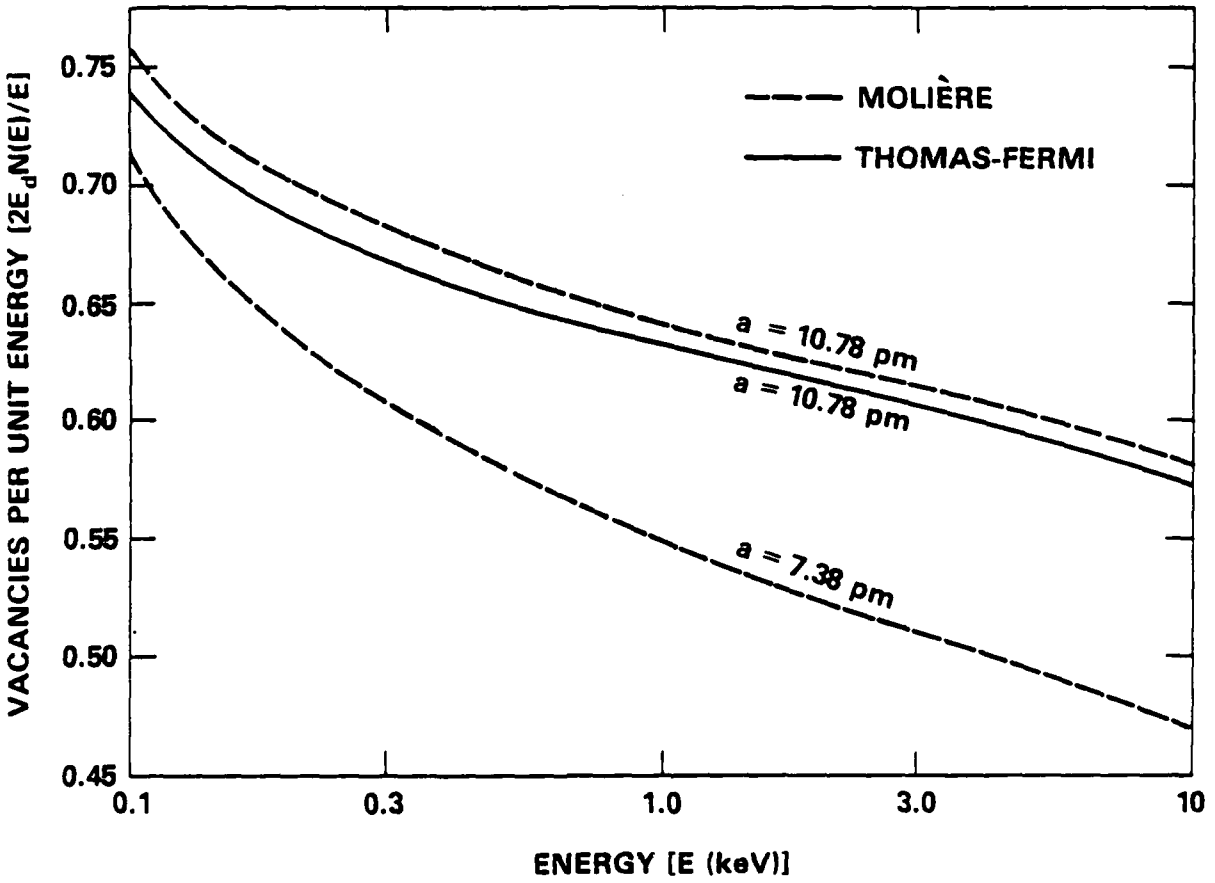

Fig. 6 -- A comparison of the number of vacancies produced for the same three cross sections as the last figure.

fig. 5 and fig. 6, we fail to see any clear relation between damage energy and number of vacancies, relative to changes in the potential.

We can examine this disparity by looking at other properties of the cross sections. In fig. 7 we show the ratio of the total elastic stopping power to the electronic stopping power for each of the three potentials. The total elastic stopping is given by

$$S_N(E) = \int_0^E dT \; T \; \Phi_N(E,T) \; . \qquad (24$$

Clearly, the reason that the Thomas-Fermi interaction leads to greater damage energy than does the Molière is that the elastic stopping dominates the electronic to a much greater extent in the Thomas-Fermi case. We note that the WSS cross section and the Molière (each with the 10.78 pm screening length) lead to the same stopping at high energies, as we would expect. But the

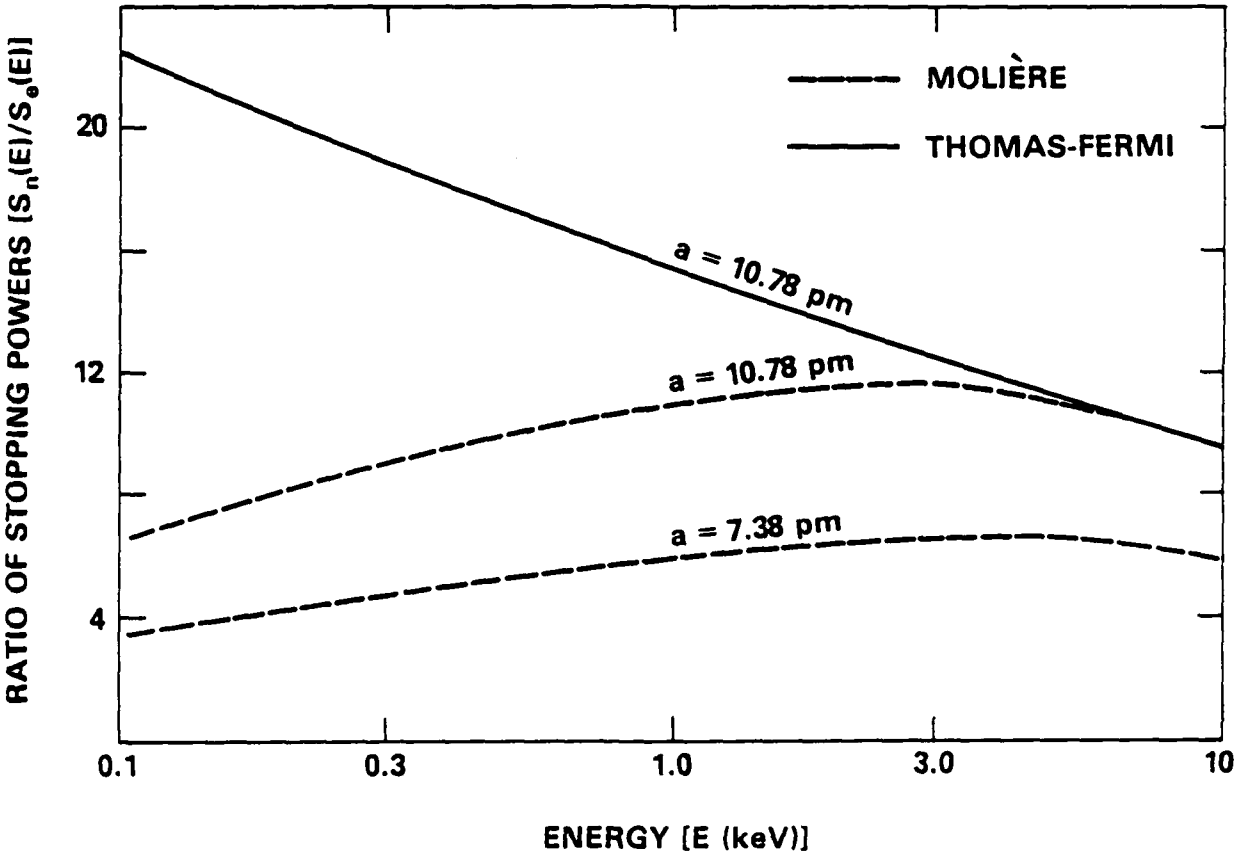

Fig. 7 -- A comparison of the ratio of nuclear and inelastic stopping powers for the same three cross sections as fig. 5.

corresponding damage energy curves do not merge. The relative amounts of elastic and inelastic loss depends sensitively on the behavior of the many cascade atoms moving with lower energies, for which the disparity in relative stopping power is still felt.

BINDING AND CUTOFF EFFECTS

In fig. 8 we show the effect of introducing a binding energy of 10 eV on the various measures of damage. (This is an unnaturally large value, but it serves to indicate tendencies.) We assume that each displacement, but not replacement, costs the displaced atom 10 eV. The solid curve in fig. 8 shows the percentage reduction in the number of Frenkel pairs as a function of energy. Also shown are the percentage changes in the thermal loss H(E) and the damage energy D(E)=H(E)+B(E). We see that the imposition of a binding energy produces opposite effects in the damage energy and the number of displacements, indicating that damage energy is not a good measure of displacement production.

The imposition of a finite cutoff energy makes no change in the number of Frenkel pairs produced, but the asymptotic value of the damage energy fraction is reduced by 18 percent and

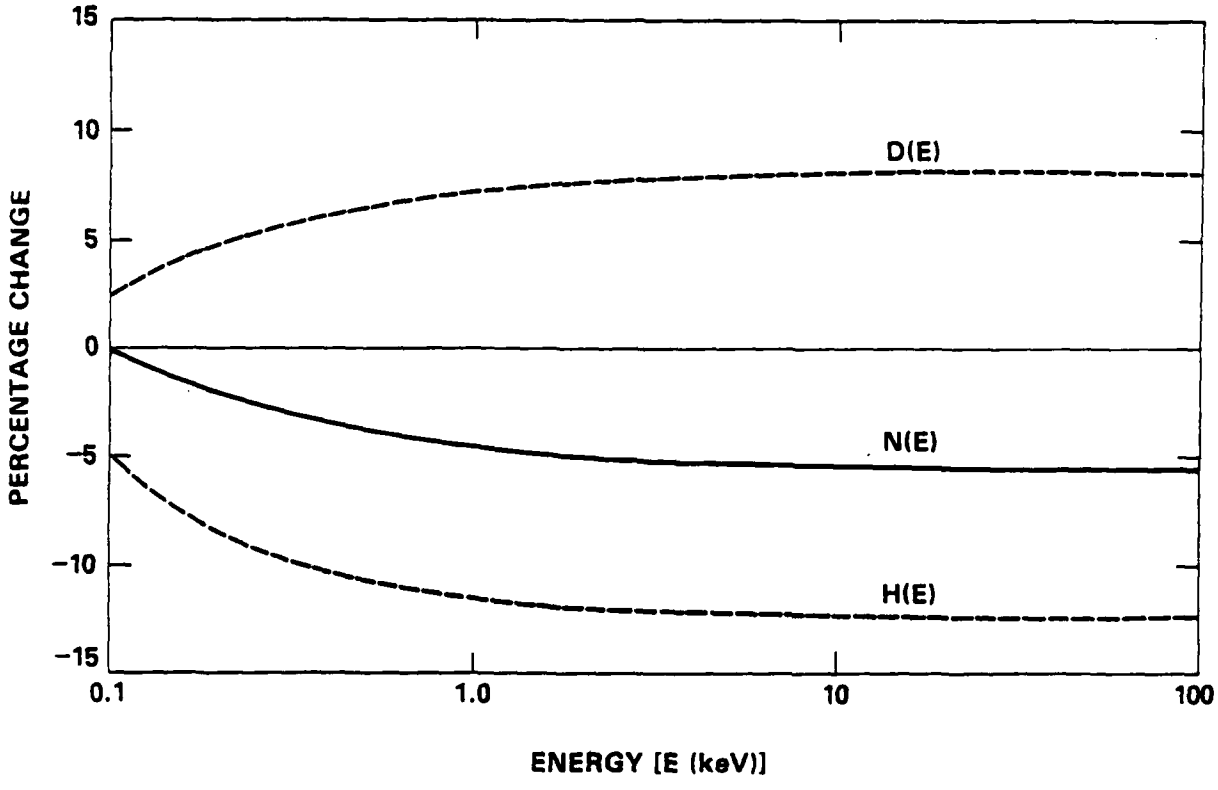

Fig. 8 -- The percentage change in the number of vacancies, damage energy and thermal losses when a 10 eV binding energy is imposed.

25 percent when the cutoff energy is 25 eV and 50 eV, respectively. This is another example that the estimates of the number of vacancies and of the damage energy are sensitive to different effects.

COMPARISON TO LNST

Our formalism coincides with that of LNST when E_C, E_B and E_D are zero, in which case our integral equation for D(E) is identical to the LNST equation for damage energy. In the absence of a finite displacement energy, we would naively expect that there would be no damage energy, because all of an ion's energy would eventually be drawn off by collisions with the electrons. LNST find, however, that if the inelastic stopping goes to zero as E^p and if the interatomic potential falls off as r^{-s}, then there is a non-zero solution of the damage energy equation provided that $s<2/(1-p)$. (In fact, the value of s should not be very close to the limit.) For the standard velocity-proportional inelastic stopping, this requires $s<4$. LNST use the Lindhard, Nielsen and Scharff cross section, which is a form of the Thomas-Fermi cross section that has the low energy behavior equivalent to $s=3$. In order to effect a comparison with LNST, we use the WSS fit to the LNS cross section (see Appendix C, eq. (C1) and eq. (C8)) and the LNST electronic stopping (eqs. (C15-C17)).

In fig. 9 we compare our results for the fraction of energy that is damage energy. The LNST curve is the equal mass result of Winterbon,[26] plotted as a function of the reduced energy value $\epsilon=E/E_L$ (Eq. (C4)). The present theory is represented by three curves, for three different values of $\epsilon_D=E_D/E_L$. (The limited extent of the $\epsilon_D=5\times10^{-7}$ curve is due to a numerical quirk in the code that was not worth removing for the sake of this one demonstration.) For definiteness, in the case of copper the specific values of the displacement energy corresponding to the the three curves are 0.14 eV, 14 eV and 1400 eV. Even in the case of the tiny 0.14 eV displacement energy, there is a marked difference between our results and the $E_D=0$ results of the LNST method.

The LNST results are always noticeably lower than the present results. The reason for this is that in our approach, for energies below E_D, certain modes of energy loss are prohibited. Most ions with energies below E_D are tied to lattice sites, either by way of having been a lattice atom that received a subthreshold energy transfer or because they arrived at a lattice site as a replacement. In both cases, in our model, they are incapable of losing energy to electronic processes. In the LNST model ions continue to lose energy electronically until they have zero energy. This effect is insensitive to changes in the displacement energy. When we halve the displacement energy, we roughly double the number of displaced atoms, each of whose energy eventually drops below the new E_D value and is prohibited from losing energy electronically. It is this prohibited loss mechanism in the present approach that accounts for the qualitative difference between the curves in fig. 9.

In closing this section, we note that there are other ways to estimate a damage energy without imposing restrictions on the low energy behavior of the interatomic potential. Miller and

Boring,[27] for instance, require that the inelastic stopping vanish at low energies, of the the order of the ionization energies of the electrons. As in our model, this condition prohibits inelastic losses below certain energies and guarantees a finite damage energy.

CONCLUSIONS

The present theory yields good estimates of displacement damage when compared to the binary-collision simulation code MARLOWE. Agreement is quite good when MARLOWE is run in its amorphous mode using the modified cross section that is used by the present approach. But even when these allowances are not made, the present theory differs from MARLOWE by less than 10 percent in the case (fcc copper) we examined. Changes in interatomic potential have a much different effect on the damage energy, which is widely used to estimate displacement damage, than they do on a direct calculation of the number of displacements. Similarly, a finite binding energy creates differing responses in the two approaches.

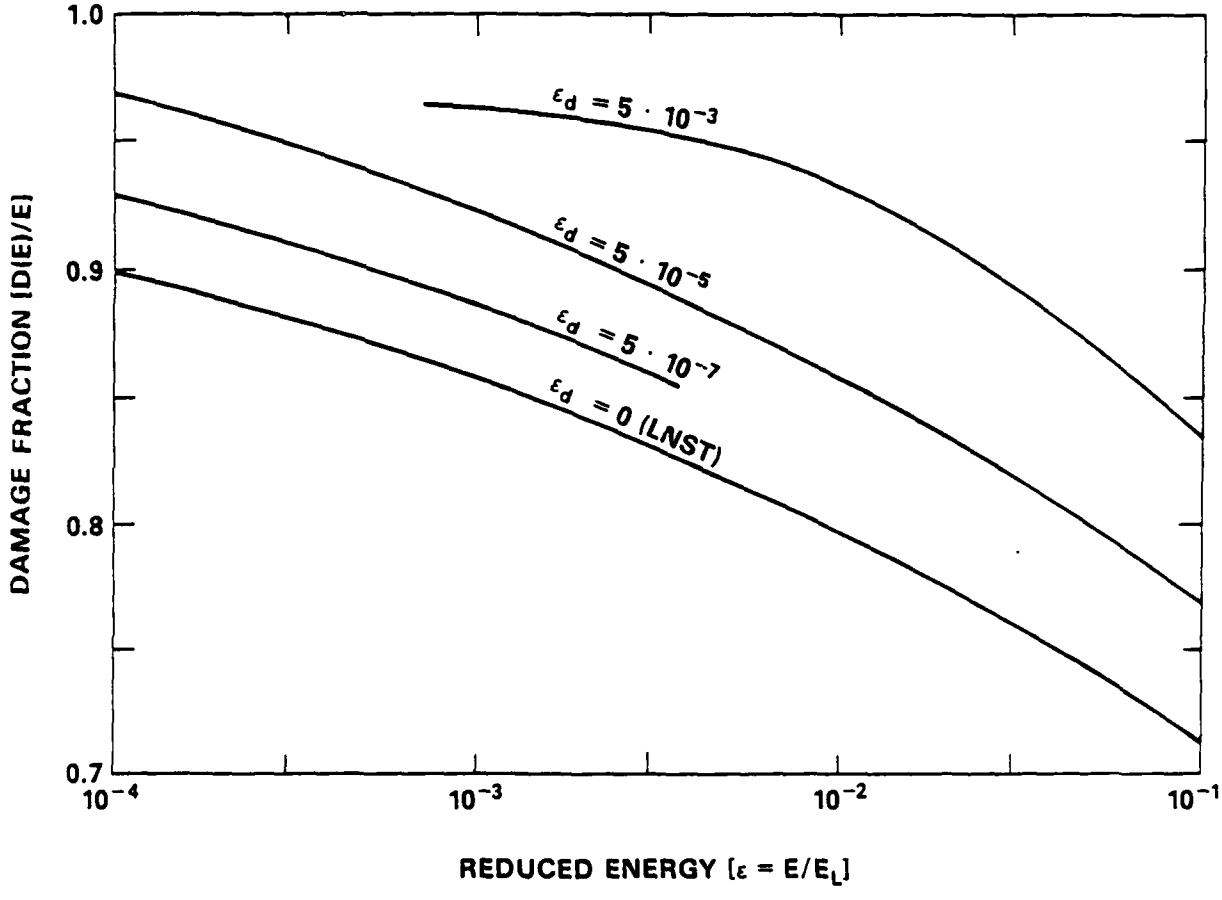

Fig. 9 -- A comparison of the damage fraction as a function of energy for a variety of displacement energies.

Finally, we have noted that any evaluation of the damage energy requires some restriction on the relative strength of the inelastic and elastic cross sections at low energies. LNST assume a very soft low-energy elastic cross section, whereas we assume that atoms bound to the lattice suffer no inelastic loss. We again find that these differences in the models create large differences in the estimates of damage energy.

We conclude that the direct calculation of the displacement production is considerably more reliable than estimating it from the damage energy.

Acknowledgments

I would like to thank Mervine Rosen for several suggestions that improved the manuscript.

APPENDIX A: DERIVATION OF THE OTHER INTEGRAL EQUATIONS

In the same manner that the integral equation for $N_V(E)$ was derived in Section 3, we can develop the equivalent integral equations for the other quantities of interest. We can let $F_i(E)$ ($i=R,B,T,E$) stand for the quantities $N_R(E)$, $B(E)$, $H(E)$, and $I(E)$, repsectively. Then $F_{i,j}(E,T)$ represents the residual quantity $F_i(E,T)$ that appears when a collision occurs under the influence of the j cross section, $j=V,R,T,E$. The only non-zero $F_{i,j}(E,T)$ are

$$
\begin{aligned}
F_{V,V} &= 1 \\
F_{R,R} &= 1 \\
F_{B,V} &= E_B \\
F_{T,T} &= T \\
F_{T,R} &= E-T \\
F_{E,E} &= T \, .
\end{aligned}
\tag{A1}
$$

The form (19) can be used to represent the integral equation for $F_i(e)$,

$$
[\, S_E(E) + S_T(E) \,]\, F_i'(E) \;+\; \Phi_{RD}(E)\, F_i(E) \;+\; J_i(E) \;=\; G_i(E) \tag{A2}
$$

where $G_i(E)$ is the integral expression

$$
G_i(E) = \int_0^E dT \;\{\, \Phi_R(E,T)\, F_i(T) \;+\; \Phi_V(E,T)\, [\, F_i(E-T) + F_i(T-E_B) \,] \,\}\,, \tag{A3}
$$

and the appropiate inhomogeneous term for these are

$$
J_i(E) = -\Phi_R(E),\; -S_B(E),\; -S_T(E)-S_R(E),\; -S_E(E), \tag{A4}
$$

for $i=R,B,T,E$. We note that if the equations for B(E), H(E) and I(E) are added, we obtain an integral equation for $F(E)=B(E)+H(E)+I(E)$ that is satisfied by $F(E)=E$.

APPENDIX B: TEST OF THE THERMAL STOPPING APPROXIMATION

In order to assess the accuracy of the thermal stopping approximation we consider its effect on the calculation of I(E). Replacing the integral

$$\int_0^{E_0} dT \;\; \Phi_T(E,T) \;\; [\; I(E) - I(E-T) \;]$$

by $S_T(E)\, I'(E)$ will clearly be least accurate for $E<E_0$. For energies of this order we can easily obtain the first few terms of a power series solution[28] of the integral equation for I(E). Using the WSS (Winterbon, Sigmund and Sanders)[18] form of the LNS[24] version of the Thomas-Fermi cross section (see Appendix C, Eq. (C1) and Eq. (C8)), and using the LNST[12] electronic stopping (Eqs. (C15-16)), both solutions can be written (in the equal mass case) in the form

$$I(E) / E = a_1 s + a_2 s^2 + a_3 s^3,$$

$$s = (2k/\lambda)\,(E/E_L)^{1/6} \qquad \text{(B1}$$

where E_L is the Lindhard energy unit (eq. (C4)), k is the electronic stopping coefficient (Eq. (C15)), and λ=1.309 appears in the WSS cross section. We find that the coefficients (a_1, a_2, a_3) are (0.5973, -0.3794, 0.2543) for the present theory without the thermal stopping approximation and are (0.5714,-0.3333, 0.1975) with the approximation. The form (B1) should only be used for energies less than the displacement energy, due to the discontinuity in the second derivative of I(E) at $E=E_0$.

When we use typical values of E_0 and examine elements from beryllium to uranium, we find a systematic error in I(E) of about 4 percent at $E=E_0$ due to the thermal stopping approximation. The error for energies less than E_0 is only slightly larger. It should be negligible at higher energies. This error is certainly less than other inaccuracies associated with this type of displacement damage calculation, so we are justified in using the thermal stopping approximation.

APPENDIX C: SPECIFIC CROSS SECTIONS AND POTENTIALS

The most commonly used cross section for atomic scattering problems is the LNS[24] version of the Thomas-Fermi cross section. By using what we will call the LNS method,[23] they obtain a simple, universal, cross section based on the Thomas-Fermi potential. They write the cross section as

$$\Phi_N(E,T)\, dT = n \pi a^2 s^{-2} f_L(s)\, ds , \tag{C1}$$

$$s^2 = E\, T / (\gamma E_L^2) , \tag{C2}$$

$$\gamma = 4 A_1 A_2 / (A_1+A_2)^2 , \tag{C3}$$

$$E_L = Z_1 Z_2 e^2 (A_1 + A_2) / (a A_2) \tag{C4}$$

$$a = [2(3\pi/32)^{2/3}]\ [\hbar^2/(me^2)]\ Z^{-1/3} = 0.8853\ a_0\ Z^{-1/3} , \tag{C5}$$

$$Z = Z_L = (Z_1^{2/3} + Z_2^{2/3})^{3/2} . \tag{C6}$$

where n is the number density of the atoms in the substrate. The LNS screening length depends on their choice of $Z=Z_L$. Another common choice is that of Firsov,[29]

$$Z = Z_F = (Z_1^{1/2} + Z_2^{1/2})^2 . \tag{C7}$$

LNS supply the kernel of their cross section, $f_L(s)$, in tabular form. More convenient is the fit to f_L by WSS, in the form[18]

$$f_W(s) = \lambda s^{1/3} [1 + (2 \lambda s^{4/3})^{2/3}]^{-3/2} , \lambda = 1.309 . \tag{C8}$$

The Molière potential is[20]

$$V(r) = [Z_1 Z_2\ e^2 / r]\ \chi_M(r/a) . \tag{C9}$$

$$\chi_M(x) = 0.35 \exp(-0.3x) + 0.55 \exp(-1.2x) + 0.10 \exp(-6x) \tag{C10}$$

One can follow the LNS method and obtain the cross section equivalent (within the assumptions of the LNS method) to this potential. This cross section has been fit to a convenient form[22]

$$f_M(s) = \begin{cases} (0.007 + s/2) / (0.0387 + 0.826\, s + s^2) , & s>s^*=.06 \\ -s\ 20.45 \ln(s) - 71\, s + 422.097\, s^2 - 1429.70\, s^3 , & s<s^* \end{cases} \tag{C11}$$

In order to use the LNS approximate form of the Molière cross section in the code MARLOWE, we make use of the relation between the impact parameter and the energy transfer given by

$$(p/a)^2 = \int_{s^*}^{\infty} ds\ s^{-2}\ f(s) \qquad \text{(C12}$$

where

$$s^* = (E\ T^*\ /\ \gamma\ E_L^{\,2})^{1/2}\ . \qquad \text{(C13}$$

Given the value of s^* in eq. (C12) corresponding to p/a, we can determine the energy transferred T^* in the collision from eq. (C13). The scattering angle is then given by

$$\theta = 2\ \sin^{-1}\ (T^*/\gamma E)^{1/2}\ . \qquad \text{(C14}$$

We note that we also set the apsis of the collision equal to the impact parameter, which is a part of the LNS approximation.

The LNST[12] expression for of the electronic stopping (eq. (6)) is

$$S_E(E) = k_L\ E^{1/2}\ , \qquad \text{(C15}$$

$$k_L = .7323\ \ n\ \ Z_1^{7/6}\ Z_2\ Z_L^{-1}\ A_2^{-1}\ A_1^{-1/2}\ eV^{1/2}\ \text{Å}^{-1}\ . \qquad \text{(C16}$$

where n is in units of gm/cm^3 and the masses in amu. The equivalent Firsov expression can be obtained from Eqs. (16-19) of Ref. 9; it also has the form (C15) with

$$k_F = .2024\ \ n\ \ (\ Z_1 + Z_2\ )\ A_2^{-1}\ A_1^{-1/2}\ eV^{1/2}\ \text{Å}^{-1}\ . \qquad \text{(C17}$$

REFERENCES

1. A.R. Knudson, et al, IEEE Trans. Nuclear Science NS-32 (85) 4388.

2. G.P. Summers, et al, IEEE Trans. Nuclear Science NS-34 (87) 1134.

3. G.J. Dienes and G.H. Vineyard, Radiation Effects in Solids (Interscience, New York, 1957) pp. 1-32.

4. A. Sosin and W. Bauer, Studies in Radiation Effects in Solids, Vol. 3, Ed. G.J. Dienes (Gordon and Breach, New York, 1969) pp. 153-327.

5. M.T. Robinson, in Radiation Induced Voids in Metals, Atomic Energy Commission Symposium Series No. 26, Eds. J.W. Corbett and L.C. Ianniello (U.S. Atomic Energy Commision, Oak Ridge, 1972), pp. 397-429.

6. Chr. Lehmann, Interaction of Radiation with Solids and Elementary Defect Production (North-Holland, New York, 1977).

7. J. Gittis, Irradiation Effects in Crystalline Solids (Applied Science Publishers, London, 1978) pp. 1-36.

8. R.S. Averback and M.A. Kirk, Surface Alloying by Ion, Electron, and Laser Beams, Eds. L.E. Rehn, S.T. Picraux, and H. Wiedersich (American Society for Metals, Metals Park, Ohio, 1986, pp. 91-135.

9. M.T. Robinson and I.M. Torrens, Phys. Rev. B9 (1974) 5008.

10. M.T. Robinson and O.S. Oen, J. Nucl. Mater. 110 (1982) 147.

11. See, for instance, Ref. 3, p. 18, or Ref. 5, p. 409.

12. J. Lindhard , V. Nielsen , M. Scharff and P.V. Thomson, K. Dan. Vidensk. Selsk., Mat. Fys. Medd. 33 (1963) No. 10.

13. P. Sigmund, Phys. Scripta 28 (1983) 257.

14. M.J. Norgett , M.T. Robinson and I.M. Torrens, Nucl. Sci. Eng. 33 (1975) 50.

15. G.P. Mueller, Nuc. Inst. Meth. 170 (1980) 389.

16. C.A. Coulter and D.M. Parkin, J. Nucl. Mater. 95 (1980) 193.

17. P. Sigmund , M.T. Mathies and D.L. Phillips, Rad. Eff. 11 (1970) 39.

18. K.B. Winterbon, P. Sigmund and J.B. Sanders, K. Dan. Vidensk. Selsk., Mat. Fys. Medd. 37 (1970) No. 14.

19. G.P. Mueller and M. Rosen, U. S. Naval Research Laboratory Memorandum Report 3942 (1979).

20. G. Molière, Z. Naturofrsch. 2a (1947) 133.

21. M.T. Robinson, Phys. Rev. 179 (1969) 327.

22. G.P. Mueller, Rad. Eff. Lett. 50 (1980) 87.

23. G.P. Mueller, U. S. Naval Research Laboratory Memorandum Report 5624 (1985).

24. J. Lindhard , V. Nielsen and M. Scharff, K. Dan. Vidensk. Selsk., Mat. Fys. Medd. 36 (1968) No. 10.

25. I.M. Torrens and M.T. Robinson, Radiation Induced Voids in Metals, Atomic Energy Commission Symposium Series No. 26, eds. J.W. Corbett and L.C. Ianniello (U.S. Atomic Energy Commision, Oak Ridge, 1972), pp. 739-756.

26. K.B. Winterbon, Ion Implantation Range and EnergyDeposition Distributions, Vol. 2, (IFI/Plenum, New York, 1975), p. 199.

27. M.S. Miller and J.W. Boring, Phys. Rev. A9 (1974) 2421.

28. K.B. Winterbon, Rad. Eff. 13 (1972) 215.

29. O.B. Firsov, Sov. Phys. JETP 6 (1958) 534.